Influence of three-dimensional dynamics on the training effect in ferromagnet-antiferromagnet bilayers

Paolo Biagioni,* Antonio Montano,† and Marco Finazzi
LNESS, Dipartimento di Fisica, Politecnico di Milano, Piazza Leonardo da Vinci 32, 20133 Milano, Italy
(Received 10 April 2009; revised manuscript received 19 July 2009; published 1 October 2009)

Training effect in exchange-bias systems consists of a variation in coercivity and symmetry between the first reversal after field cooling and the following loops. It has been shown, in the frame of a two-dimensional coherent-rotation approach, that training might be explained in terms of an initial noncollinear arrangement of the antiferromagnetic spins after field cooling, which relaxes to a collinear arrangement during the first reversal [A. Hoffmann, Phys. Rev. Lett. **93**, 097203 (2004)]. In this paper, we extend the model to three dimensions, by numerically solving the Landau-Lifshitz-Gilbert equation describing the precession motion of magnetic moments. We are thus able to discuss the validity of Hoffmann's model within a three-dimensional approach, with parameter values similar to those in the original publication, and to enlighten the role of out-of-plane anisotropies and Gilbert damping in determining the occurrence of training. Moreover, when realistic values are considered for the magnetocrystalline anisotropy of the system, we find that no training is reproduced within our extended model, suggesting that symmetry-driven irreversibilities might not be as relevant as previously believed for training effect.

DOI: 10.1103/PhysRevB.80.134401 PACS number(s): 75.40.Mg, 75.60.Ej, 75.60.Jk, 75.70.Cn

I. INTRODUCTION

Magnetization reversal in bilayer systems constituted by a ferromagnet (FM) and an antiferromagnet (AFM) is often characterized by a shift and by enhanced coercivity in the hysteresis loop. This effect, known as exchange bias (EB), finds fundamental applications in the field of magnetic-data storage and has originated a large debate and a flourishing of publications in the attempt to give it a firm description.[1]

While it is now widely recognized, both experimentally and theoretically, that EB mechanisms must be described at a microscopic level by taking the detailed spin structure at the interface and inside the AFM into account,[2–9] some peculiar features of magnetization reversal have been proposed to depend mainly on the average exchange and anisotropy energies, which are well described even within the frame of macroscopic coherent-rotation models.

An important example is given by the training effect (TE), resulting in a different coercivity and a change in symmetry between the first reversal after field cooling and the following loops.[10–19] It has been suggested that two mechanisms can contribute to this phenomenon: on the one hand, in some polycrystalline samples, TE seems to be connected with the domain microstructure in the EB system and with thermally activated depinning of AFM spins, as corroborated by experimental and numerical results.[15,19] On the other hand, experiments reveal that in some systems TE can be independent on the crystalline quality of the film.[13] Hoffmann has shown[20] that this observation might be related to the anisotropy symmetry properties of the magnetic films and interpreted in terms of a difference in the arrangement of the macroscopic magnetic moments in the AFM between the initial condition right after field cooling (noncollinear arrangement) and all the following configurations (collinear arrangement): while the first loop begins with the system in its minimum-energy configuration, which could be reached by surmounting energy barriers during field cooling, all the following loops lead to a metastable configuration, which modifies the symmetry and coercivity of reversal in the FM layer. This mechanism is fully determined by exchange and anisotropy energies in the system, within a macroscopic description of magnetic moments, and has been reproduced by minimizing the total energy of the system as a function of the applied field. However, two approximations represent a possible limit to the application of such a model:[20] (i) the system is treated by assuming an infinite in-plane anisotropy, fully confining the moments in the plane of the film and (ii) the values chosen for the in-plane magnetocrystalline anistropy of the AFM, when compared with the exchange energies, are roughly two to three orders of magnitude larger than those in realistic EB systems.

One of the most intriguing aspects of hysteresis-loop simulation in EB systems are the very different results that are sometimes obtained when minimization algorithms are compared with calculations where the full Landau-Lifshitz-Gilbert (LLG) equation is solved to describe precession of the magnetic moments. A remarkable example is given in a paper by Schulthess and Butler,[21] who showed how Koon's model for FM-AFM interfaces[22] is not a good description for EB when moment precession, rather than energy minimization, is taken into account. There is a fundamental reason for this: EB reversal dynamics, as also evident in Hoffmann's model for TE, develops in an energy landscape which shows many local energy minima. In this situation, the transient dynamics of magnetic moments, i.e., their path toward equilibrium, can largely influence the final local energy minimum where the system falls. Different paths lead to a different ability of overcoming energy barriers and therefore to different final steady states.[23] The simulation of a magnetic moment preceding around an effective field therefore allows the system to reach new final states, which could not be reached by means of simple in-plane rotation.

In the frame of this discussion, an important issue is to extend Hoffmann's model for symmetry-driven TE, where

the interplay between local and global minima plays a key role, to a three-dimensional (3D) description for the evolution of the FM-AFM system by means of LLG equations. A recent paper by Saha and Victora[24] already applies LLG dynamics to a polycrystalline FM-AFM bilayer composed of noninteracting, randomly oriented grains. Their paper highlights the role of micromagnetic domain evolution on EB and TE. However, the presence of many grains while making the system more realistic, partially conceals the role of anisotropy in the TE. Indeed, for some parameter values, they find training even in the case of uniaxial magnetocrystalline anisotropy in the AFM, at variance with Hoffmann's model, probably due to the many degrees of freedom made available by the randomly oriented grains.

In this work we simulate the behavior of an FM-AFM bilayer by solving the LLG equation. In the first part of the paper, we show that the LLG equation can indeed reproduce TE within a three-dimensional extension of Hoffmann's macroscopic model, when an initial in-plane noncollinear arrangement of the AFM moments is considered and as long as parameter values similar to those in the original manuscript are chosen. In doing this, we also enlighten some differences which emerge in the magnetic-moment configurations. In particular, the presence of a finite out-of-plane anisotropy opens a new channel for AFM spin relaxation by out-of-plane reorientation, which turns out to be strictly connected with the occurrence of training. To further enlighten the key role of the precession motion, we also show how changes in the Gilbert damping constant can as well rule the occurrence of training, by determining different paths toward equilibrium.

In the second part of the paper, we choose the system parameters, particularly the magnetocrystalline anisotropy in the AFM, in order to better adhere to the properties of realistic EB bilayers. In doing so we find that, although noncollinear initial conditions can still be obtained, they now possess a large out-of-plane component. When hysteresis loops are then simulated by solving the LLG equations, no training is observed anymore, a hint that symmetry-driven effects might be responsible for TE only in the limit of very large magnetocrystalline anisotropy.

II. MODEL

The system under study is an FM/AFM bilayer, modeled following Ref. 20 in the frame of a coherent-rotation approach as an ensemble of three magnetic moments $\mathbf{M}_F$, $\mathbf{M}_{AF1}$, and $\mathbf{M}_{AF2}$, the first one describing the FM layer and the other two for the two sublattices representing the AFM layer (see Fig. 1). The total energy of the system can be written as the sum of Zeeman, anisotropy, and exchange (AFM exchange and interface exchange) contributions

$$E_{tot} = E_{Zeeman} + E_{anisotropy} + E_{exchange}. \tag{1}$$

The temporal evolution of each magnetic moment $\mathbf{M}_i$ is described by the LLG equation[25–27]

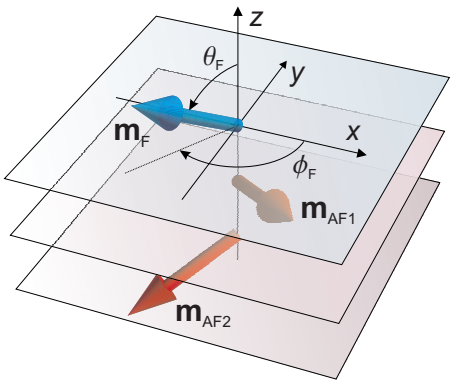

FIG. 1. (Color online) Sketch of the simulated FM-AFM system with the polar coordinate system used throughout the paper.

$$\frac{d\mathbf{M}_i}{dt} = -\gamma \mathbf{M}_i \times \mathbf{H}_i + \frac{\alpha}{|\mathbf{M}_i|}\mathbf{M}_i \times \frac{d\mathbf{M}_i}{dt}, \tag{2}$$

where γ is the gyromagnetic ratio of the electron spin, α is the Gilbert damping constant, and $\mathbf{H}_i$ is the effective field acting on the ith magnetic moment, defined as

$$\mathbf{H}_i = -\frac{\partial E_{tot}}{\partial \mathbf{M}_i}. \tag{3}$$

A normalized LLG equation can then be written by substituting $\mathbf{m}_i = \mathbf{M}_i/|\mathbf{M}_i|$ and $\tau = \gamma t$. Hence the system dynamics is fully determined once the damping constant α and the total energy E_{tot} are provided. The latter can be written by considering the following expressions:

$$E_{Zeeman} = -\sum_i \mathbf{H}_0 \cdot \mathbf{M}_i; \tag{4a}$$

$$E_{anisotropy} = \sum_i |\mathbf{M}_i| \left[-\frac{1}{2}k_{1,i}(m_{i,x}^4 + m_{i,y}^4 + m_{i,z}^4) + k_{2,i}m_{i,y}^2 + k_{3,i}m_{i,z}^2 \right]; \tag{4b}$$

$$E_{exchange} = -\sum_{i \neq j} J_{i,j}\mathbf{M}_i \cdot \mathbf{M}_j, \tag{4c}$$

where $\mathbf{H}_0$ is the external applied field, $k_{1,i} > 0$ and $k_{2,i} < 0$ are anisotropy constants describing cubic and uniaxial magnetocrystalline anisotropy, respectively, $k_{3,i} > 0$ describes in-plane anisotropy due to both shape anisotropy (for the FM) and interface anisotropy associated to the removal of inversion symmetry in a layered structure (for both FM and AFM moments), and finally $J_{i,j}$ is the exchange coupling constant between the ith and the jth magnetic moment. The exchange coupling energy contains the AFM exchange coupling ($J_{AF1,AF2} < 0$) and the interface exchange coupling of the FM layer with the first ($J_{F,AF1} > 0$) and the second ($J_{F,AF2} > 0$) AFM sublattice. As the effect of a finite temperature is not included in the model, results must be interpreted as a zero-temperature limit.

In order to implement a numerical solution for the LLG equation, a suitable constraint must be imposed to numeri-

cally ensure conservation of the magnitude of magnetic moments during their evolution. A natural choice is to rewrite the normalized LLG equation in polar coordinates, which automatically guarantees $|\mathbf{m}|=1$. The vectorial LLG equation (three equations, three unknowns for each moment) is thus replaced by the following system (two equations, two unknowns for each moment, see Fig. 1):

$$\frac{d\vartheta}{d\tau} + \alpha \frac{d\varphi}{d\tau} \sin\vartheta = -h_x \sin\varphi + h_y \cos\varphi; \tag{5a}$$

$$-\alpha \frac{d\vartheta}{d\tau} + \frac{d\varphi}{d\tau} \sin\vartheta = h_z \sin\vartheta - (h_x \cos\varphi + h_y \sin\varphi)\cos\vartheta. \tag{5b}$$

This finally yields a system of six nonlinear, strongly intertwined ordinary differential equations, which is solved by means of a multistep adaptive algorithm based on numerical differentiation formulas of order 5.[28]

In order to provide the numerical code with suitable initial conditions, mimicking the state of the system after field cooling, we find the absolute minimum-energy configuration, for a given set of parameters, by means of a global search heuristic method, namely, a genetic algorithm, because of the occurrence of many local minima.[29,30] After each iteration, a fast deterministic algorithm is used to refine the search before fitness evaluation.

III. SIMULATIONS FOR LARGE MAGNETOCRYSTALLINE ANISOTROPY

In this section we simulate the FM-AFM system under study with parameter values in the range of those used by Hoffmann.[20] As a suitable initial condition for each loop simulation, the minimum-energy configuration of the magnetic moments for a given set of parameters must be calculated, in order to reproduce the state of the system after field cooling. Such an initial condition has already been derived by Hoffmann in the two-dimensional limit of very large AFM cubic magnetocrystalline anisotropy (AFM moments always aligned along an easy axis) and no FM magnetocrystalline anisotropy (FM moment always aligned with the applied field).[20] His results show the occurrence of three different regimes as a function of magnitude and direction of the applied field, namely, parallel, antiparallel, and noncollinear (perpendicular) in-plane arrangements of the two AFM moments $\mathbf{M}_{AF1}$ and $\mathbf{M}_{AF2}$. It is also shown that if the cubic anisotropy term is replaced by a uniaxial term in the AFM then the noncollinear phase disappears. It seems to be implicit in the paper that whenever the system is found in the noncollinear phase after field cooling then its evolution is characterized by training in the FM hysteresis loop.

We first test our genetic algorithm within a two-dimensional energy description (i.e., fixing $\vartheta=90°$ in our model) in order to reproduce the phase-diagram analytically calculated by Hoffmann but with finite anisotropy values. We use $J_{F,AF1}=J_{F,AF2}=-0.4J_{AF1,AF2}$, $k_{1,F}=-0.1J_{AF1,AF2}M_F$, $k_{1,AF1}=k_{1,AF2}=-0.4J_{AF1,AF2}M_F$, no uniaxial anisotropy ($k_{2,i}=0$), and in-plane anisotropy only for the FM layer ($k_{3,F}=-J_{AF1,AF2}M_F$, $k_{3,AF1}=k_{3,AF2}=0$). We indeed reproduce the trend already obtained by Hoffmann, just with slightly shifted boundaries between different phases (see Fig. 2). We also find, in agreement with Ref. 20 that the presence of uniaxial anisotropy prevents the stabilization of a noncollinear AFM configuration (not shown).

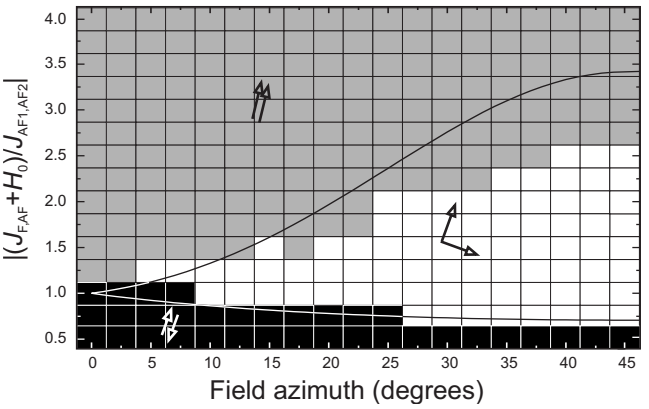

FIG. 2. Results from two-dimensional energy minimization with the genetic algorithm (gray-scale boxes) and comparison with Hoffmann's analytical model (solid line). The arrows represent the arrangement of the two AFM sublattices. Each box is the result of one simulation with parameter values corresponding to the center of the box. White, gray, and black boxes correspond to in-plane noncollinear, parallel, and antiparallel arrangements, respectively.

We then include the ϑ degree of freedom in our description and maintain the same parameters as above. In doing this, we find again that three phases are present (see Fig. 3), however the antiparallel phase now corresponds to a configuration where the two AFM moments have their main projections along the out-of-plane anisotropy axis with just a small canting ($<30°$ with respect to the polar axis). This out-of-plane configuration can be attributed to the inherent in-plane frustration determined by the competition between

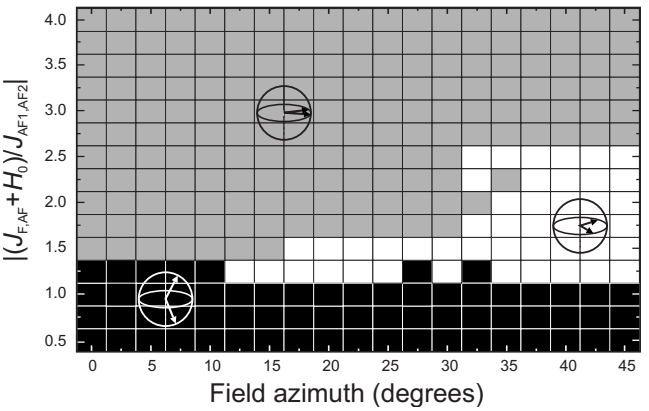

FIG. 3. Results from three-dimensional energy minimization with the genetic algorithm. The arrows represent the arrangement of the two AFM sublattices. Each box is the result of one simulation with parameter values corresponding to the center of the box. White, gray, and black boxes correspond to in-plane noncollinear, in-plane parallel, and out-of-plane antiparallel arrangements, respectively. In the out-of-plane antiparallel arrangement, a small canting is present, as described in the text.

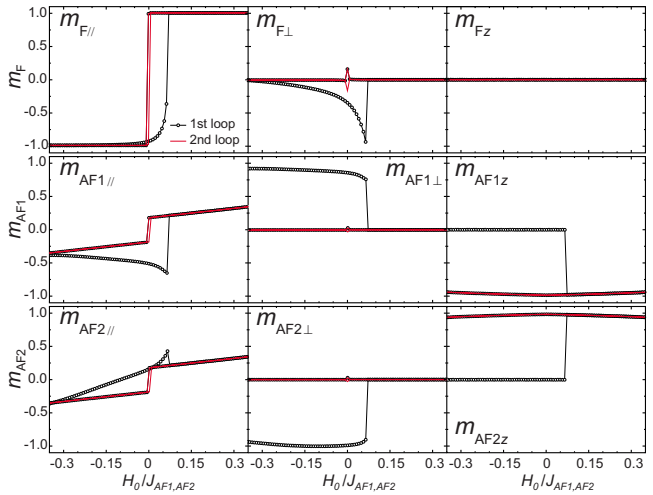

FIG. 4. (Color online) Results from LLG simulations of TE. For each magnetic moment the three components are shown, namely, the in-plane component parallel (∥) to the applied field, the in-plane component perpendicular (⊥) to the applied field, and the out-of-plane (z) component. The hysteresis loop is covered twice.

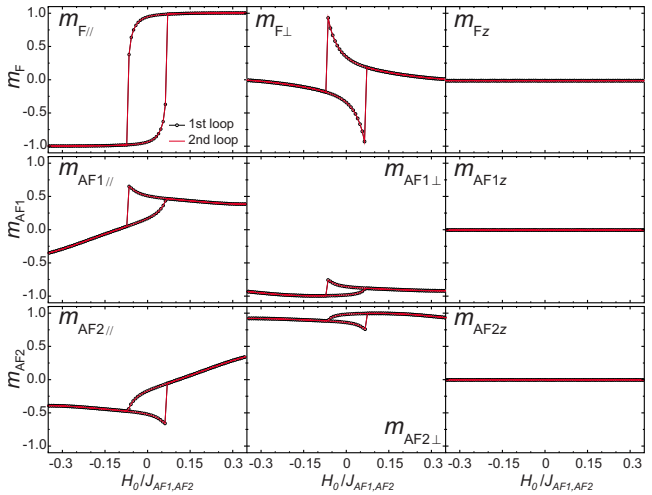

FIG. 5. (Color online) Results from LLG simulations with in-plane anisotropy for the AFM layers. All other parameters are the same as in Fig. 4. For each magnetic moment the three components are shown, namely, the in-plane component parallel (∥) to the applied field, the in-plane component perpendicular (⊥) to the applied field, and the out-of-plane (z) component. The hysteresis loop is covered twice.

AFM exchange coupling and interface exchange coupling, which is relaxed in the out-of-plane arrangement. Also the two in-plane parallel and antiparallel phases show a small canting with respect to the anisotropy axes.

Within our extension of Hoffmann's model to three dimensions, we simulate training by first applying the minimization genetic algorithm to find the system energy minimum, in order to describe the configuration of magnetic moments after field cooling. We then cover the whole hysteresis loop twice (from negative fields to positive fields and back) in order to evaluate the occurrence of training. For each field value, the LLG equations are solved numerically by taking the configuration obtained at the end of the previous step as initial condition and finally obtaining the new steady-state arrangement. The typical integration time for each step, chosen in order to fully reach a steady state, is $\tau \simeq 10\,000$, while we use $\alpha=0.1$ as a damping constant. This damping value will be modified later on in order to discuss its influence on the simulation results.

Representative hysteresis loops are shown in Fig. 4, calculated starting from an initial condition of noncollinear arrangement for the two AFM sublattices (white area of the phase diagram in Fig. 3). We indeed find that, for parameter values similar to those presented by Hoffmann in his examples, TE is well reproduced (see panel $m_{\mathrm{F}\parallel}$ in Fig. 4). All the situations where we have occurrence of training do not qualitatively differ from this one. Loops are simulated with the same set of parameters used for Fig. 3. The field is applied in the plane of the sample with a $\varphi=20°$ tilt with respect to the cubic anisotropy axis. In the figure we show the three components for each of the three magnetic moments involved in the simulations, namely, the two components in the plane of the sample (parallel and perpendicular to the applied field, respectively) and the one perpendicular to the sample surface. By looking at the out-of-plane component of the two AFM moments (see panels $m_{\mathrm{AF1}z}$ and $m_{\mathrm{AF2}z}$ in Fig. 4), it is clearly seen that during the first half loop they lay in the plane of the sample, while their main projection is along the surface normal during the whole following evolution. This relaxation from an in-plane to an out-of-plane arrangement takes place during the first FM reversal and can be attributed to the already mentioned in-plane frustration determined by the interplay between AFM and interface exchange.

Such an out-of-plane relaxation is a peculiar feature emerging from our model and it appears to be strictly connected with the occurrence of training. In order to prove this, we show in Fig. 5 simulation results obtained with the same parameters and same initial conditions as in Fig. 4 but with an in-plane anisotropy term added to the two AFM sublattices ($k_{3,\mathrm{AF1}}=k_{3,\mathrm{AF2}}=-J_{\mathrm{AF1,AF2}}M_{\mathrm{F}}$), preferentially confining them in the sample plane. It is clearly seen that now the evolution of the AFM moments is fully confined in the plane of the sample (see panels $m_{\mathrm{AF1}z}$ and $m_{\mathrm{AF2}z}$ in Fig. 5) and that this is accompanied by no training (see panel $m_{\mathrm{F}\parallel}$ in Fig. 5). Such a behavior highlights that not only the symmetry of the in-plane anisotropy but also its out-of-plane component

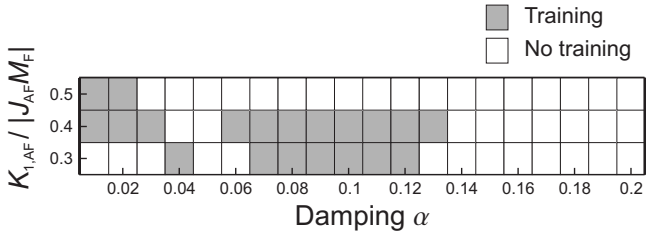

FIG. 6. Graph showing the occurrence of training for a FM-AFM bilayer as a function of the damping coefficient α and for three different values of the AFM cubic anisotropy constants $k_{1,\mathrm{AF1}}=k_{1,\mathrm{AF2}}$. All other simulation parameters are the same as those used for the simulation shown in Fig. 4.

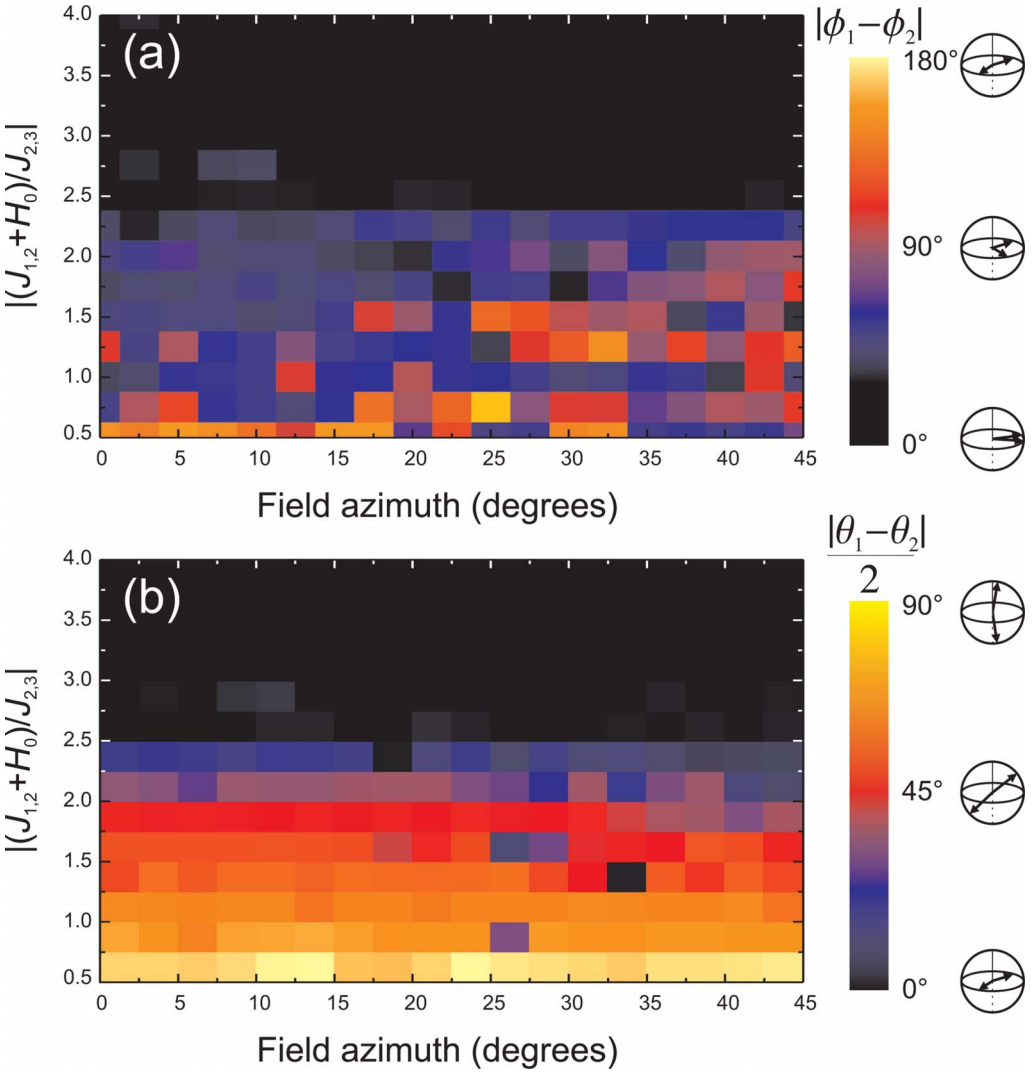

FIG. 7. (Color online) Results from three-dimensional energy minimization with the genetic algorithm, for a system with realistic magnetocrystalline anisotropy (see text): (a) azimuthal angle $|\varphi_1-\varphi_2|$ between the two in-plane projections of the AFM moments and (b) average polar tilt $|\vartheta_1-\vartheta_2|/2$ of the two AFM moments. The arrows nearby the color bar are a sketch of the AFM moment geometry.

might play a significant role in determining the occurrence of training.

It should then be stressed that, within our approach based on LLG equations, an in-plane noncollinear arrangement of the two AFM magnetic moments after field cooling is a necessary but not sufficient condition for the occurrence of training. We indeed find that for several combinations of parameter values, for which we can find a cooling field leading to an initial AFM noncollinear arrangement, nontrained loops are nevertheless obtained. This can be attributed to the peculiar spiral-like path of the transient moment dynamics, leading to a different ability of overcoming energy barriers compared with simulations based on energy minimization. This finding is in full analogy with the analysis by Schulthess and Butler[21] about Koon's model for FM-AFM interfaces,[22] where the introduction of LLG equations extended the original results showing new possible regimes.

As already pointed out, in such complex systems, such as FM-AFM interfaces, where the interplay between local and global minima plays an important role in the system dynamics, different transient spatial paths can lead to very different final steady states. This is also true when the evolution is changed by modification in the damping constant α. A larger damping value shrinks the spiral-like evolution of the magnetic moments and therefore makes again different final-energy minima available. This is clearly shown in Fig. 6, where we analyze the occurrence of training as a function of the damping constant α for three different values of the AFM cubic anisotropy constants $k_{1,\mathrm{AF1}}=k_{1,\mathrm{AF2}}$. As a lower value for α determines a longer characteristic evolution time for the system, we increase the value of τ accordingly, in order to ensure that a steady-state configuration is always reached. All other simulation parameters are the same as the ones used for the simulation in Fig. 4. The relevance of this finding is evident when considering that many common factors can influence the damping constant, for example, the size of a magnetic device,[31] impurities,[32–34] or its operating temperature.[35,36] It should also be pointed out that, in FM/AFM LLG simulations, care is often taken in order to ensure that the results are independent of the value of the damping

parameter.[21,24] While this might be the case for a single FM structure, our findings show that in the dynamics of a FM/AFM bilayer the damping constant might play a relevant role in determining the local minimum reached during the reversal dynamics.

IV. SIMULATIONS FOR SMALL MAGNETOCRYSTALLINE ANISOTROPY

As briefly discussed in the introduction, the parameter values used in Hoffmann's model, where all exchange and anisotropy energies are of the same order of magnitude, might be a poor description for many experimentally relevant systems showing EB and TE. If we restrict ourselves to the case of CoO/Co bilayers, as in Ref. 20, the magnetocrystalline anisotropy constant takes a value of about 2×10^5 erg/cm^3,[37] corresponding to roughly 2×10^{-6} eV/atom once the lattice parameter of CoO is taken into account. On the other side, typical values for the exchange integrals are 2×10^{-4} eV/atom and 2×10^{-3} eV/atom for the nearest-neighbor 90° exchange and the second-neighbor 180° exchange, respectively.[38] Therefore, in a realistic model the exchange energy should be two to three orders of magnitude larger than the magnetocrystalline anisotropy. As for the AFM coupling at the interface between the FM layer and the two AFM sublattices, it has been evaluated, assuming Heisenberg exchange across the interface, to be on the order of 1 meV/nm^2.[39] In order to be used in our model, where all the spins of each sublattice are represented by a single magnetic moment, such a value should be scaled down by the number of atomic layers constituting the film, which might be of some tens to some hundreds. Therefore, the interface exchange energy is also expected to be two to three orders of magnitude lower than the AFM exchange coupling.

According to the discussion above, we run new simulations for the initial conditions after field cooling, by means of the genetic algorithm. All parameter values are the same as before, except for the AFM magnetocrystalline anisotropy and the interface exchange coupling, which are set to $k_{1,\mathrm{AF1}}=k_{1,\mathrm{AF2}}=-0.01J_{\mathrm{AF1,AF2}}M_{\mathrm{F}}$ and $J_{\mathrm{F,AF1}}=J_{\mathrm{F,AF2}}=-0.01J_{\mathrm{AF1,AF2}}$, respectively.

The results are shown in Fig. 7. Due to the low magnetocrystalline anisotropy, the phase diagram now shows a number of configurations where the AFM moments are not aligned close to any of the anisotropy axes. Therefore, to better convey the complex 3D arrangement, we plot both the angle $|\varphi_1-\varphi_2|$ between the in-plane components of the two AFM moments [panel (a)] and the angle $|\vartheta_1-\vartheta_2|/2$ [panel (b)], which for AFM moments laying on opposite sides with respect to the equatorial plane (which is the case with our set of parameters) provides the average polar tilt of the AFM moments with respect to such a plane.

A close inspection of the results from energy minimization reveals that many noncollinear situations are again obtained but mostly with moment orientation not aligned with any of the anisotropy axes. We have extensively analyzed the hysteresis loops simulated with LLG equations starting from such initial conditions and found that no sign of TE is ever obtained. This result is a hint that, for realistic systems where the magnetocrystalline anisotropy is much lower than the AFM exchange, symmetry-driven contributions to TE might be less relevant than previously believed.

V. CONCLUSIONS

In conclusion, we have extended Hoffmann's model for symmetry-driven TE in FM-AFM bilayers to three dimensions, by numerically solving the LLG precession equation for the magnetic moments. For the same parameter values as those used by Hoffmann, we verify that even within our extended three-dimensional model the occurrence of training is strictly connected with the configuration of AFM magnetic moments after field cooling. Some peculiar new features of the training dynamics anyway emerge in our analysis. First of all, the transition during the first FM reversal is accompanied by an out-of-plane relaxation of the two AFM moments, driven by the inherent in-plane frustration between interface and AFM exchange. This enlightens that the out-of-plane anisotropy can play a key role in the occurrence of training. Moreover, an initial noncollinear AFM arrangement is a necessary but not sufficient condition for training, whose dynamics strongly depend also on other system parameters. In particular, when realistic values are chosen for the exchange and anisotropy energies, TE is not reproduced anymore within our model, suggesting that symmetry-driven irreversibilities might not be as relevant as previously believed for TE in realistic systems where the magnetocrystalline anisotropy is much lower than the AFM exchange.

All such considerations confirm that the behavior of FM-AFM interfaces can be very complex even within a coherent-rotation approach based only on three magnetic moments and that therefore not only the symmetry-driven initial state after field cooling plays a role for TE but also the dynamics of the magnetic moments as governed by anistropy, interface coupling, and damping.

ACKNOWLEDGMENTS

We warmly acknowledge L. Duò for discussions and for his continuous support.

*paolo.biagioni@polimi.it

†Present address: Edison s.p.a., Foro Buonaparte 31, 20121 Milano, Italy.

[1] For review articles, see J. Nogués and I. K. Schuller, J. Magn. Magn. Mater. **192**, 203 (1999); A. E. Berkowitz and K. Takano, *ibid.* **200**, 552 (1999); M. Kiwi, *ibid.* **234**, 584 (2001).

[2] A. P. Malozemoff, Phys. Rev. B **35**, 3679 (1987); **37**, 7673 (1988); J. Appl. Phys **63**, 3874 (1988).

[3] U. Nowak, K. D. Usadel, J. Keller, P. Miltényi, B. Beschoten, and G. Güntherodt, Phys. Rev. B **66**, 014430 (2002).
[4] J. Keller, P. Miltényi, B. Beschoten, G. Güntherodt, U. Nowak, and K. D. Usadel, Phys. Rev. B **66**, 014431 (2002).
[5] U. Nowak, A. Misra, and K. D. Usadel, J. Magn. Magn. Mater. **240**, 243 (2002).
[6] F. Nolting, A. Scholl, J. Stöhr, J. W. Seo, J. Fompeyrine, H. Siegwart, J.-P. Locquet, S. Anders, J. Lüning, E. E. Fullerton, M. F. Toney, M. R. Scheinfeink, and H. A. Padmore, Nature (London) **405**, 767 (2000).
[7] A. Scholl, M. Liberati, E. Arenholz, H. Ohldag, and J. Stöhr, Phys. Rev. Lett. **92**, 247201 (2004).
[8] M. Finazzi, Phys. Rev. B **69**, 064405 (2004).
[9] M. Finazzi, P. Biagioni, A. Brambilla, L. Duò, and F. Ciccacci, Phys. Rev. B **72**, 024410 (2005).
[10] H. Xi, R. M. White, S. Mao, Z. Gao, Z. Yang, and E. Murdock, Phys. Rev. B **64**, 184416 (2001).
[11] A. Hochstrat, C. Binek, and W. Kleemann, Phys. Rev. B **66**, 092409 (2002).
[12] W. T. Lee, S. G. E. te Velthuis, G. P. Felcher, F. Klose, T. Gredig, and E. D. Dahlberg, Phys. Rev. B **65**, 224417 (2002).
[13] L. Malkinski, T. O'Keevan, R. E. Camley, Z. Celinski, L. Wee, R. L. Stamps, and D. Skrzypek, J. Appl. Phys. **93**, 6835 (2003).
[14] S. Brems, D. Buntinx, K. Temst, C. Van Haesendonck, F. Radu, and H. Zabel, Phys. Rev. Lett. **95**, 157202 (2005).
[15] S. Brems, K. Temst, and C. Van Haesendonck, Phys. Rev. Lett. **99**, 067201 (2007).
[16] M. S. Lund and C. Leighton, Phys. Rev. B **76**, 104433 (2007).
[17] T. Hauet, S. Mangin, J. McCord, F. Montaigne, and E. E. Fullerton, Phys. Rev. B **76**, 144423 (2007).
[18] P. Y. Yang, C. Song, F. Zeng, and F. Pan, Appl. Phys. Lett. **92**, 243113 (2008).
[19] M. K. Chan, J. S. Parker, P. A. Crowell, and C. Leighton, Phys. Rev. B **77**, 014420 (2008).
[20] A. Hoffmann, Phys. Rev. Lett. **93**, 097203 (2004).
[21] T. C. Schulthess and W. H. Butler, Phys. Rev. Lett. **81**, 4516 (1998).
[22] N. C. Koon, Phys. Rev. Lett. **78**, 4865 (1997).
[23] B. Dieny and J. P. Gavigan, J. Phys.: Condens. Matter **2**, 187 (1990).
[24] J. Saha and R. H. Victora, Phys. Rev. B **73**, 104433 (2006).
[25] L. Landau and E. Lifshitz, Phys. Z. Sowjetunion **8**, 153 (1935).
[26] T. L. Gilbert, Armour Research Foundation Report No. A059, 1956 (unpublished).
[27] T. L. Gilbert, IEEE Trans. Magn. **40**, 3443 (2004).
[28] L. F. Shampine and M. W. Reichelt, SIAM J. Sci. Comput. (USA) **18**, 1 (1997).
[29] T. Bäck, *Evolutionary Algorithms in Theory and Practice: Evolution Strategies, Evolutionary Programming, Genetic Algorithms* (Oxford University Press, New York, 1996).
[30] A. R. Conn, N. Gould, and Ph. L. Toint, Math. Comput. **66**, 261 (1997).
[31] D. Steiauf and M. Fähnle, Phys. Rev. B **72**, 064450 (2005).
[32] J. O. Rantschler, R. D. McMichael, A. Castillo, A. J. Shapiro, W. F. Egelhoff, B. B. Maranville, D. Pulugurtha, A. P. Chen, and L. M. Conners, J. Appl. Phys. **101**, 033911 (2007).
[33] W. Bailey, P. Kabos, F. Mancoff, and S. Russek, IEEE Trans. Magn. **37**, 1749 (2001).
[34] C. Scheck, L. Cheng, I. Barsukov, Z. Frait, and W. E. Bailey, Phys. Rev. Lett. **98**, 117601 (2007).
[35] B. Heinrich, D. J. Meredith, and J. F. Cochran, J. Appl. Phys. **50**, 7726 (1979).
[36] J. F. Cochran and B. Heinrich, IEEE Trans. Magn. **16**, 660 (1980).
[37] M. J. Carey, A. E. Berkowitz, J. A. Borchers, and R. W. Erwin, Phys. Rev. B **47**, 9952 (1993).
[38] K. Tomiyasu, T. Inami, and N. Ikeda, Phys. Rev. B **70**, 184411 (2004).
[39] F. T. Parker, K. Takano, and A. E. Berkowitz, Phys. Rev. B **61**, R866 (2000).